

## Very high altitude micro air vehicle deployment method

P.Burdziakowski\*, L.Galecki\*\*, M.Mazurkiewicz\*\*\*, J.Struzinski\*\*\*\*

\*Faculty of Civil and Environmental Engineering, Gdansk University of Technology, Narutowicza 11/12, 80-233 Gdansk, Poland (email: [pawel.burdziakowski@wilis.pg.edu.pl](mailto:pawel.burdziakowski@wilis.pg.edu.pl))

\*\*III Liceum Ogólnokształcące im. Marynarki Wojennej RP in Gdynia, ul. Legionow 27, 81-405 Gdynia, Poland (e-mail: [lukasz.b.galecki@gmail.com](mailto:lukasz.b.galecki@gmail.com))

\*\*\*III Liceum Ogólnokształcące im. Marynarki Wojennej RP in Gdynia, ul. Legionow 27, 81-405 Gdynia, Poland (e-mail: [mateusz.a.mazurkiewicz@gmail.com](mailto:mateusz.a.mazurkiewicz@gmail.com))

\*\*\*\*III Liceum Ogólnokształcące im. Marynarki Wojennej RP in Gdynia, ul. Legionow 27, 81-405 Gdynia, Poland (e-mail: [jashorpl@gmail.com](mailto:jashorpl@gmail.com))

---

**Abstract:** The paper presents the original work and method for high altitude micro air vehicle deployment. The method is based on the scientific ballooning, and adapted for stratospheric flight of commercial off-the-shelf micro air vehicle in flying wing configuration. The High Altitude Micro Air Vehicle, built for this research, was deployed during a test experiment at the lower level of the stratosphere. The results of the experiment and technical details are presented. The paper concludes the experiment's findings and delivers assumptions for the future work and next experiment.

© 2019, IFAC (International Federation of Automatic Control) Hosting by Elsevier Ltd. All rights reserved.

**Keywords:** autonomous vehicles, autonomous control, aerospace engineering, micro air vehicle, deployment, microbiology, microbes, Mars

---

### 1. INTRODUCTION

High-altitude platforms (HAPs) are aircraft positioned above an altitude of 20 km, in the stratosphere. Stratospheric flights provide new, extensive opportunities for human activity in the areas like: commercial flights, military applications, scientific measurements, and experiments. There is a wide range of applications for stratospheric flights that can be conducted by unmanned aerial vehicles. It can be stated that the most valuable applications for society are weather forecasting, investigation of stratospheric dynamics processes, tracking the origins and movements of polluting emissions, crop and forest assessments, monitoring of wildlife migration, volcanic eruptions and ocean currents, observation of highway traffic patterns (Goraj, Frydrychiewicz, & Winiecki, 1999). Other, especially military applications are not considered in this paper, however the potential is very big as well. The presented system has been developed, manufactured and tested especially for microbiology experiments. The stratospheric flights may be conducted by airplanes, airships or balloons, either manned or unmanned. The stratosphere is the layer of the atmosphere where the temperature starts to increase with altitude. Immediately after the tropopause, which has a constant temperature of about  $-60^{\circ}\text{C}$ , the stratosphere starts at an altitude of 7 km at the poles and 18 km at the Equator, extending to around 50 km (D'Oliveira, Melo, & Devezas, 2016).

The presented system can be classified to the very high altitude vehicles (Epley, 1997). Due to the fact that, the highest altitude achieved by an electrically powered unmanned aircraft is 29 524 m by the NASA Helios (Noll et al., 2007), and is the highest altitude in horizontal flight by a

winged aircraft, the researches decided to employ scientific ballooning techniques to build a hybrid UAV and its deployment method, in order to overcome the barrier of propeller-powered aircraft, and simultaneously use the advantages of both technologies. The interdisciplinary method presented in the paper improves both deployment of the MAV (Micro Air Vehicle) to the highest possible altitude, and scientific ballooning payload recovery. The method can be used in both cases and in applications requiring very or extremely high-altitude flight and precise payload recovery.

As of the publication of this paper, the presented high-altitude micro air vehicle system has been deployed and reached highest possible altitude for electric motor propelled unmanned micro air vehicle in flying wing configuration, and finally has successfully automatically landed on the launch site, using the on-board flight controller, without human operator intervention.

#### 1.1 Background of the study

The main inspiration for the research described in (D. J. Smith et al., 2014) was the problem of scarcity of suitable flight systems for microbiological upper atmosphere experiments. The researchers designed and built a self-contained payload for exposing microorganisms in the stratosphere, launched on a large scientific balloon. Conducting experiments on microbes at extreme altitudes may help predict their response on the surface of Mars. In the same context, the research (Beck-Winchatz & Bramble, 2014) shows the outline of the experiments carried out by students. Typical flights of the balloons used last for 2.0-2.5 hours and reach altitudes of approximately 30 km. Payloads with plant seeds and yeast are exposed to intense cosmic and

ultraviolet radiation, temperatures below  $-60^{\circ}\text{C}$ , and atmospheric pressures of approximately 0.01 atmospheres. The main reason for studying plant seeds exposed to the conditions of space is the fact that the ability to grow plants will likely be crucial for the success of future long-duration spaceflight and for the habitation on the Moon and Mars (Beck-Winchatz & Bramble, 2014). Technically, the system is based on a payload with a GPS tracker, carried by a scientific balloon. In both cases, the payload is recovered by airdropping the cargo which has a parachute attached. In general this method of recovering the payload is well known within the scientific ballooning community (Epley, 1997; Jones, 2007; Pagitz, 2007; Rainwater & Smith, 2004; M. Smith & Rainwater, 2013; Yajima, Izutsu, Imamura, & Abe, 2009). Despite the fact that scientific ballooning is the method that provides the highest possible altitude for that kind of experiment, without using specialized spacecraft, the payload recovery or landing phase has some dysfunctions. On the other hand, there is possibility to use high altitude aircrafts, either manned or unmanned, which are free of that dysfunction. The payload recovery is safe, due to the fact that the high altitude aircraft lands in a controlled manner. Unmanned airplanes are able to operate at a maximum altitude of around 30 km (D'Oliveira et al., 2016), however the cost of an airplanes and its dimensions are very big. Moreover, airplanes designed for high-altitude operation are very prone to any atmospheric disturbances (winds, thermals) during the start and landing phases, due to the fact that aerodynamically, the airplanes are adapted to operate at high altitude in a low density atmosphere. Some of the projects that suffered problems during start phase, finally ended with crashes (National Transportation Safety Board, 2015) (Noll et al., 2007). The optimized structures for high-altitude flights have the disadvantage of fragility at gust conditions found at lower altitudes (D'Oliveira et al., 2016).

The main idea for this study was to build a low-cost micro air vehicle, able to be deployed at the 30 km mark, with an experimental payload. It should have the ability to automatically land at take-off position (home position), after a short operation period at the very high altitude, or at a point chosen by the operator. In order to reach this goal, a hybrid method has been developed and the high altitude micro air vehicle (HAMAV) has been built.

## 2. METHOD DESCRIPTION

The very high altitude micro air vehicle deployment method consists of following phases (Fig. 1): system deployment, high altitude lift, detachment, low air density falling, controlled flight, landing.

The system deployment is the initial phase of the method. In this phase the system is technically prepared for the flight. The balloon (a lifter) is prepared for flight, the HAMAV is connected to the lifter, the aerial system is connected to the communication module and the entire system is tested (motors, navigation, radio control link, video link, telemetry link, releasing mechanism). Then, the payload module is loaded with biological samples.

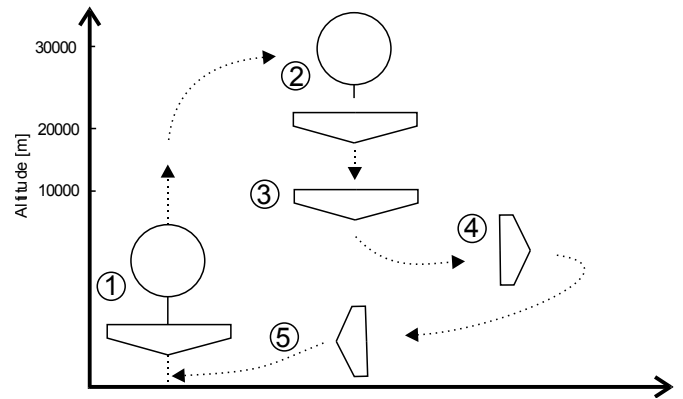


Fig. 1 Very high altitude micro air vehicle deployment method phases: high altitude lift (1), detachment (2), low air density falling (3), controlled flight (4), landing (5)

### 2.1 Very High Altitude Lift

Very high altitude lift is the first flying phase of the presented method. After the system has been deployed and tested on the ground, the lifting phase is started. The HAMAV is connected to the lifter (scientific balloon) using the novel releasing system. The lifting is constantly monitored via telemetry link, to control the altitude and platform position. In case the lifter drifts out of the selected lifting zone or the HAMAV reaches its final altitude, the flight controller will automatically release the aircraft from the balloon. The operator can release the HAMAV manually at any point in time.

### 2.2 Low air density falling

The low density falling phase is started, after the detaching phase is set in motion. The releasing mechanism is triggered, the HAMAV is detached and starts to fall. The low density air is insufficient for complete maneuverability of the platform during the first seconds of the phase, until the MAV reaches sufficient speed to generate wing lift. The minimal speed required to generate lift has been calculated using methodology described in (Dionis, Liviu, & Ileana, 2018) and the vortex lattice method (VLM) for the sea level, 12 000 m and 30 000 m AGL. The "U.S. Standard Atmosphere 1976" parameters for the atmosphere were used. The "U.S. Standard Atmosphere 1976" is an atmospheric model of how the pressure, temperature, density, and viscosity of the Earth's atmosphere changes with altitude. The vortex lattice method (VLM), is a numerical, computational fluid dynamics method used mainly in the early stages of aircraft design. The VLM models the lifting surfaces, such as a wing, of an aircraft as an infinitely thin sheet of discrete vortices to compute lift and induced drag. As the calculation results show (for the fixed lift method), the wing used is controllable, and reaches a lift force equals to the plane's weight at 12 km AGL and 29 m/s speed ( $v$ ) at  $\alpha=5^{\circ}$ . At 30 km AGL the required speed is 167 m/s. The bending moment generated on the main wing is presented in Fig. 3.

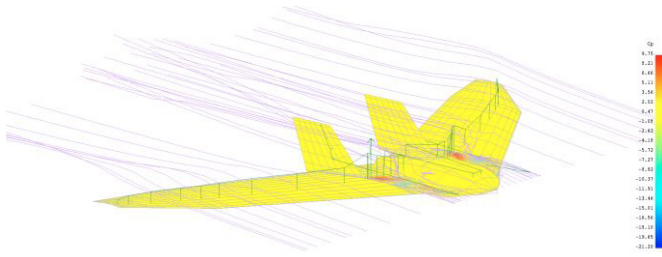


Fig. 2 Pressure Coefficient ( $C_p$ ) and stream simulation for 30 km AGL at  $\alpha=5^\circ$  ( $v=167$  m/s).

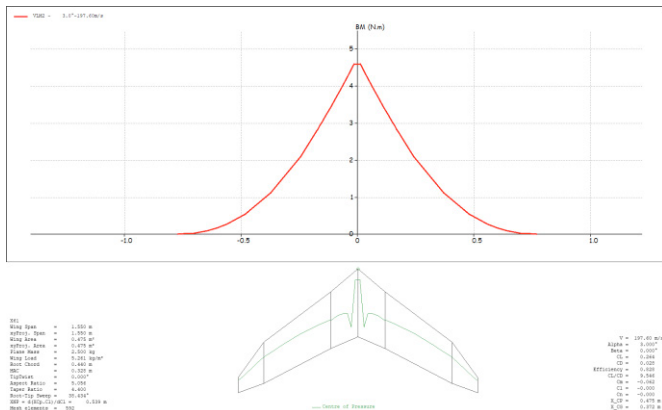


Fig. 3 Bending Moment for the flying wing configuration (enforced structure) ( $\alpha=5^\circ$ ,  $v=197$  m/s)

### 2.3 Controlled flight

The controlled flight phase is the phase where the flight controller (FC) is able to effectively regain control. The phase is started either when the air density is sufficient or the speed increases to the value at which the aerofoil will generate lift. After the FC regains control, the “back to home” command is called. The home position is saved at the start position (before the lifting phase) and the MAV starts heading towards home.

This phase is terminated at home position where the MAV lands.

## 3. SYSTEM SPECIFICATIONS

The high altitude micro air vehicle (HAMAV) system consists of following elements: high altitude platform (HAP) module, high altitude lifter (HAL) module, communication module, ground control station, payload module.

### 3.1 High altitude platform description

The high altitude platform is based on a modified commercial airframe (off-the-shelf) in a flying wing configuration, FX-61 type, with a wingspan of 1550 mm, built from EPO foam (Expanded Polyolefin foam). The platform had to be modified in order to reinforce its standard construction offered by the manufacturer, and to prepare the platform’s structure for the higher speeds and inertial forces. The structure modifications were done using 3D prints, additional carbon fiber rods and laminated fiberglass wing skin. The fiber glass and PVC tape enforces the signal and power cable

ducts. The FX-61 airframe was augmented by specially designed 3D prints. The standard components’ mounts on the fuselage have all been replaced. All of the components mounted to the EPO fuselage, including the motors, are inserted into or screwed to 3D printed parts. The main purpose for this modification was easier replacement of mounted components. In the foam based construction the manufacturer expects that the parts be inserted into the foam and glued. To avoid gluing the parts directly to the fuselage, custom 3D printed mounts are glued into the airframe, and functional components screwed to the 3D printed inserts. Some of the 3D printed parts have been designed for reducing the drag coefficient. The aerodynamic parts are designed for filling the frame’s construction slots, not used for the actual airframe configuration. The custom parts were printed from different thermoplastics using Cetus MKII and Prusa i3 MKIII 3D printers. The printing material has been selected for the intended application, mostly ABS (acrylonitrile butadiene styrene). This plastic was chosen because of its low density, high flexural modulus and impact resistance. Some parts were printed using PLA (polylactic acid) for its superior rigidity.

The power system utilizes dual energy sources. The first power source is made from LiPol (lithium-polymer) batteries in 6S2P (6 cells, 2 packs) configuration, made using Panasonic NCR 18650B (3400 mAh) battery cells. The first battery pack powers all of the on-board systems. The secondary (backup) battery pack powers only mission critical systems (all equipment except for the propulsion system and charging of the additional cameras). Additionally, all of the voltage regulators are doubled (paired). In case of any malfunction of one of the voltage regulator form the pair, the systems connected to it will continue to be powered, from the backup voltage regulator. As a result, the HAP has the ability to be controlled even when the main battery has been drained. In that case the flight can be continued in gliding mode. The propulsion system is electrical brushless motor (Quantum MT Series 4108 700KV) and an APC (Advanced Precision Composites LTD) 10x10E size propeller.

An important part of the platform for the high altitude adaptation is the addition of a heating system. The heating system’s main purpose is to maintain a constant temperature for the electronics, in order to avoid gyroscopes’ drift (temperature bias). The system uses a 12 watt flexible heating mat, controlled by an Arduino Nano module with a relay switch and a temperature sensor. The heating system is programmed to sustain  $20^\circ\text{C}$  temperature inside the electronics’ compartment.

### 3.2 Payload module

The payload modules (Fig. 4), adapted for biological experiments, are placed under the wings of the HAP. The platform is able to carry 16  $1.5\text{ cm}^3$  test tubes that in this case contain extremophiles. The modules are mounted under the wings for optimal aerodynamics. The vials are first inserted into securing frame that is then secured using screws to a second frame. The second frame is the payload slot integrated with the wing. The test tubes and their contents are exposed to the outside. The biological samples are exposed to



stratospheric conditions (temperature and sunlight), similar to experiment described in (D. J. Smith et al., 2014). The exposition to stratospheric conditions is documented by the part of the research team responsible for astrobiology. The payload container was tested during an initial flight test, at an altitude of 700 meters, and was proven to be safe and functional.

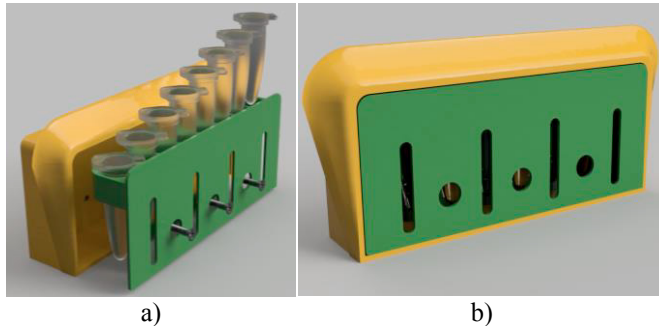


Fig. 4 The payload module with biological samples, mounted under the wing a) opened b) flight position

### 3.3 High altitude lifter module

The high altitude lifter module is based around a scientific balloon with an original releasing mechanism (Fig. 5). The novel mechanism is manufactured using servomechanism and specialized 3D printed elements, located on the aft of the MAV platform.



Fig. 5 Releasing mechanism, servo part a) open b) closed

During the lifting phase, the platform is attached to the lifter module, facing nose down, to avoid the unpredictable and uncontrollable maneuver that would have to take place upon detachment, while the HAMAV would be aligning itself to the direction of flight. Facing the platform nose down, after intentional or unintentional release, facilitates the increase of the platform's speed. Consequentiality, this causes a surge in the lift generated by the platform, making it controllable faster. The original mounting solution was invented in the form of a clamp-like polymer component that envelops the propeller, motor and part of the air frame (Fig. 6a). A line runs from the release mechanism inside the frame, through carbon fiber tubes to the back of the MAV and is secured to a cleat on the clamp. The clamp is then tied to the balloon by rope. Thanks to its unique shape and design, it stabilizes the MAV during ascent and allows quick and easy drop when the release mechanism is triggered. The clamp is manufactured using PLA plastic, which is a slow biodegrading bioplastic (Qi, Ren, & Wang, 2017), and it can begin to decompose after falling to the ground. This is important for minimizing the environmental impact of the project, since the clamp remains tied to the balloon after the HAMAV is released.

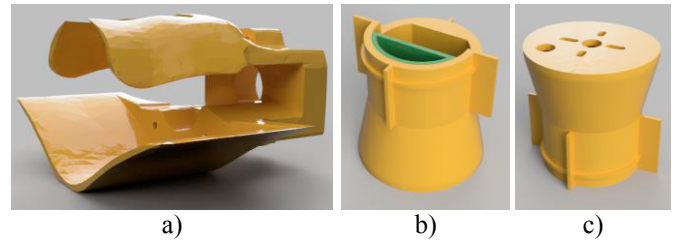


Fig. 6 Motor and platform mounting system a) platform to the balloon mount b) bottom part of motor mounting, c) top part of motor mounting

### 3.4 Communication Module

Communication is a crucial part of the system and provides the necessary information exchange between the ground control station and the platform's systems. Communication with the HAMAV takes place in two directions. Signals are sent towards the platform (uplink), and signals are received from the platform (downlink). Uplink consists of radio control (RC) signals to the MAV. Downlink provides telemetry data. The presented communication with the platform takes place within radio bands and on transmitter powers that can be used without special permission, i.e. in channels that have been allocated to the public (ISM Bands). According to the definition, the industrial, scientific and medical (ISM) radio bands are internationally recognized radio frequencies and energies for industrial, scientific and medical purposes other than telecommunications. ISM Bands allow for the use of transmitting devices without a radio license, within constrained frequencies and limited powers. In practice, this means that the released bands are very contested and available power is very limited. This fact forced the researchers to use modified and fine-tuned antenna systems, exchanging the stock dipoles.

There are three separate radio links for RC, FPV video downlink, and telemetry exchange. The stock RC system transmitter module has been exchanged for an eLeRes MAX type transmitter and a corresponding receiver has been installed on the platform. The RC working frequency band is 433MHz, which has demonstrated a 65 km range for the RC link. A Moxon type transmitting antenna has been prepared, with a gain of 5.5dB. The Moxon antenna (Moxon Rectangle) is rectangular, with half the rectangle being the driven element and the other half being the reflector. It is electrically equivalent to a two element Yagi antenna with bent elements and without directors. The Moxon Rectangle is a very simple and mechanically robust two-element parasitic array antenna. The receiving antenna is 2.2dB dipole, mounted on the platform.

The FPV link employs a LawMate transmitter and an RX-1260CK receiver. The FPV working frequency band is 1280 MHz. The transmitting antenna is a 2.2dBi dipole, while the receiving antenna is biquad 23dBi antenna. The biquad antenna is made from two single turn loop antennas forming an array, where each one is a driven component. The working principle of the biquad antenna is similar to that of a dipole antenna, generating the same radiation pattern as a dipole with more directivity and bandwidth (Yebuah & Torkudzor, 2014).

The telemetry link uses two RDF868x transceiver modules, working on the 868MHz frequency band. The stock dipoles are mounted on the platform, with a gain of 3dBi, while on the ground an SY-910 type with 11.5dBi yagi type antenna is used. The Yagi antenna (Yagi, 1997) is a directional antenna consisting of multiple parallel elements in a line, usually half-wave dipoles made of metal rods. Yagi antennas consist of a single driven element connected to the transmitter or receiver with a transmission line, and additional "parasitic elements" which are not connected to the transmitter or receiver: a so-called reflector and one or more directors.

#### 4. DEPLOYMENT EXPERIMENT

The first stratospheric experiment took place in November 2018, in the center of area no. TSA2B. A temporary Segregated Area (TSA) is an airspace temporarily segregated and allocated for the exclusive use of a particular user during a determined period of time and through which other traffic will not be allowed to transit. In order to minimize collision possibilities and air traffic disruption, the area had to be allocated to the presented experiment. TSA2B is the biggest segregated area available in Poland. Its size allowed for keeping the HAMAV within the area boundaries, in case of any unpredicted problems during the uncontrolled lifting phase.

The flight trajectory (Fig. 7) executed during the experiment, clearly shows the lifting phase (smooth and constant lift), the top altitude reached and moment of release, and finally the controlled flight phase.

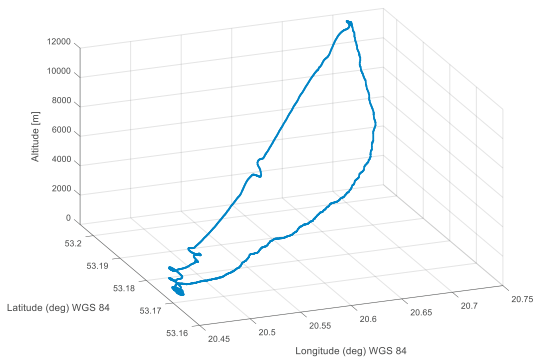


Fig. 7 Flight trajectory

Fig. 8 presents the altitude sensor's reading. The basic altitude is calculated using a barometric sensor, the ground level is assumed to be zero (BARO Alt on Fig. 8) at the start time. The AGL (Above Ground Level) latitude (AHS Alt on Fig. 8) is calculated using barometric altitude with the initial offset from GPS readings, and this AHR Alt is taken by the flight controller as the altitude taken for controlling the HAP. The GPS Altitude measured at the home position is the initial offset for AHR Altitude. The GPS altitude (GPS Alt on Fig. 8) drifted during the flight, and the difference between GPS Alt and AHR Alt was increasing. The HAMAV flight controller altimeter did not consider the appropriate atmospheric model. In that case, a proposition described in (Popowski, 2011) for altitude measurements, for that kind of

MAV, should be considered in the future work. The solution described in (Popowski, 2011) proposes an integration of three sources of information for one altitude calculation using: barometric altitude, vertical acceleration and altitude acquired the from GPS system.

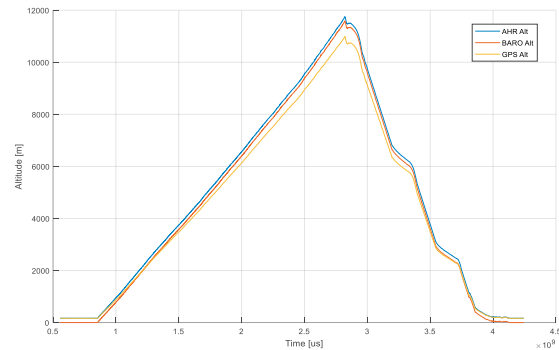


Fig. 8 Altitude sensors changes

The HAMAV speed (GPS speed) versus altitude is presented on Fig. 9. The turbulent layer of the lower part of the atmosphere up to 4000 meters initially caused speed changes and balloon trajectory variations. Above 4500 meters the speed stabilized at 10 m/s and remained at the same mean value until the release phase. After release, the platform increased its speed rapidly to 55 m/s, and after 1000 meters of controlled falling reached 80 m/s for short time (low air density falling phase). The average gliding speed varied from 20 to 40 m/s, during the controlled flight phase.

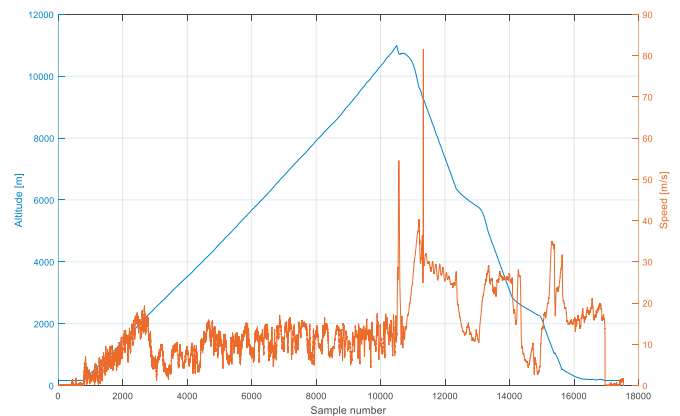


Fig. 9 Altitude and speed

The releasing phase, and initial acceleration after release does not exceeds  $30 \text{ m/s}^2$  in the Z axis, after quick stabilization to gliding position (Fig. 10). The X axis had been stabilized for the gliding position (form nose down to forward) just after the release. That behavior proves, that the atmosphere's density at 11500 meter altitude is enough to stabilize the platform, and allows the MAV to be automatically controlled by the flight controller.

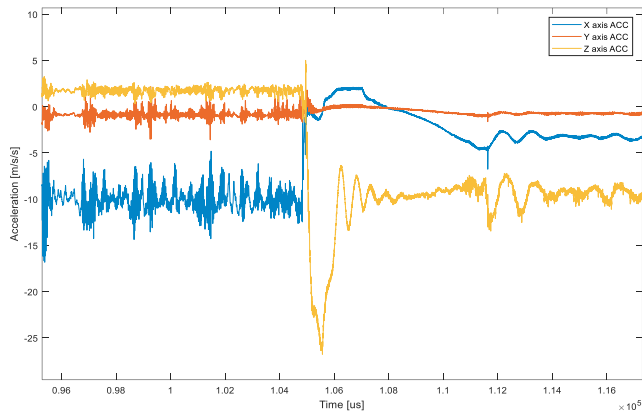


Fig. 10 Axis acceleration before and after release

On the flight during which the UAV reached the stratosphere, the test tubes contained samples of *Chlorella vulgaris*, *Fistulifera saprophila*, *Phaeodactylum tricornutum*, *Nitzschia palea* and *Chloromonas nivalis*. Samples are currently being studied by the 3-SAT astrobiology team.

## 5. RESULTS

The high altitude mission at 11,5 km, above the ground level (AGL) has been finished successfully. The mission confirmed initial assumptions and delivered some new data for the realization of the mission to the target altitude - 30km AGL.

The platform's construction, with the planned enforcements endured the low air density falling and high speed flying.

The detailed axis acceleration log analysis revealed that no aerodynamic flutter occurred during high speed flight. The flutter can occur as a result of interactions between aerodynamics, stiffness, and inertial forces on the aircraft's structure. As the speed of the air increases, there may be a point at which the structural damping is insufficient to damp out the motions which are intensifying due to aerodynamic energy being added to the structure. These vibrations can cause structural failure and therefore considering flutter characteristics was an important part of the project. As a result of this consideration, the stiffness of the platform's structure was increased. The planned structure enforcement, and used enforcing method turned out to be adequately applied.

The flight controller sensors and data filtering algorithms have proven to be resistant to the fast and rapid orientation changes and successfully stabilize the platform whenever the air density yields the possibility to do so. The experience with some commercial off the shelf (COTS) flight controllers and algorithms (Burdziakowski & Szulwic, 2016) shows that commercial flight controllers encounter problems with platform stabilization after non-uniform, rapid and significant orientation changes. The algorithms' coefficients were tuned during an initial filed test that resulted in the proper stabilization of the MAV at higher altitudes.

The high altitude lift phase revealed some oscillation problems. During the experiment, the MAV oscillated while it was hooked up to the scientific balloon. As a result the

stabilizing 3D print was designed and tested. It will be attached to the next planned experiment. The oscillations also resulted in periodic FPV signal loss. The periodic signal losses will be eliminated using an automatic antenna tracker.

## 6. CONCLUSIONS

The project proved that high altitude flights using the presented method are possible employing a modified commercial platform and commercial micro air vehicle's electronics (flight controller, motors, batteries). The communication links established with the MAV using ISM bands and modified antennas allowed the researchers to control all flight parameters, transmit the live video stream and telemetry data during the mission. The method delivers a low cost alternative for atmospheric research and measurements, biological experiments, meteorological applications, etc..

Future work is concentrated on further development of the HAMAV's construction. A bigger airframe, with a wingspan of 2000mm, would result in smaller weight to wing area ratio and therefore better gliding capabilities at high altitudes, or alternatively, it could be used to transport larger and heavier payloads. The use of four ailerons (with flaperon function, where the flaps would act as ailerons), which would increase redundancy in the case of failure of one of the servos. A bigger propeller would increase the effectiveness of the propulsion system.

The HAMAV deployment method can be adapted to MAVs without a propulsion system. The lack of a propulsion system, would significantly reduce the total weight which would increase gliding capabilities. The controlled flight phase of the presented method can be conducted without propulsion. The gliding capabilities of the flying wing enable it to safely navigate to the home position from a high altitude, even from afar.

Further weight reduction could be achieved by modifications like: substituting PET-G with ABS for 3D prints (it would reduce the weight of the 3D prints by approximately 20%), using lighter LiPol battery pack.

## ACKNOWLEDGEMENTS

The HAMAV was created within the 3-SAT aerospace project in III High School in Gdynia. The research team is very grateful to the rest of 3-SAT project team for allowing them to pursue their research. Any help and/or support received at any stage of the project is greatly appreciated. The following deserve a special mention for their contributions: III High School in Gdynia and its School Board and Parent Board, JIT Team, Pelixar S.A, Rotor, Variosteel, Copernicus Project and the Gdansk University of Technology.

## REFERENCES

- Beck-Winchatz, B., & Bramble, J. (2014). High-altitude ballooning student research with yeast and plant seeds. *Gravitational and Space Research*, 2(1).
- Burdziakowski, P., & Szulwic, J. (2016). A commercial of the shelf components for a unmanned air vehicle

- photogrammetry. In *16th International Multidisciplinary Scientific GeoConference SGEM 2016*. <https://doi.org/10.5593/sgem2016B22>
- D'Oliveira, F. A., Melo, F. C. L. de, & Devezas, T. C. (2016). High-altitude platforms- Present situation and technology trends. *Journal of Aerospace Technology and Management*, 8(3), 249–262.
- Dionis, C., Liviu, D., & Ileana, C. J. (2018). Study of Dynamic Stability a Cannard Configuration UAV. In *2018 International Conference on Applied and Theoretical Electricity (ICATE)* (pp. 1–6). <https://doi.org/10.1109/ICATE.2018.8551468>
- Epley, L. E. (1997). Stratospheric aircraft, blimps, balloons, and long endurance vehicles. *Progress in Astronautics and Aeronautics*, 172, 211–250.
- Goraj, Z., Frydrychiewicz, A., & Winiecki, J. (1999). Design concept of a high-altitude long-endurance unmanned aerial vehicle. *Aircraft Design*, 2(1), 19–44.
- Jones, W. V. (2007). Recent developments in scientific research ballooning. *Nuclear Physics B-Proceedings Supplements*, 166, 217–222.
- National Transportation Safety Board. (2015). Raport DCA15CA117.
- Noll, T. E., Ishmael, S. D., Henwood, B., Perez-Davis, M. E., Tiffany, G. C., Madura, J., ... Wierzbanski, T. (2007). *Technical findings, lessons learned, and recommendations resulting from the Helios prototype vehicle mishap*.
- Pagitz, M. (2007). The future of scientific ballooning. *Philosophical Transactions of the Royal Society A: Mathematical, Physical and Engineering Sciences*. <https://doi.org/10.1098/rsta.2007.0002>
- Popowski, S. (2011). Verification of the idea of altitude and rate of climb measurement in selected aircraft. *Transactions of the Institute of Aviation*, 143–160.
- Qi, X., Ren, Y., & Wang, X. (2017). New advances in the biodegradation of Poly (lactic) acid. *International Biodeterioration & Biodegradation*, 117, 215–223.
- Rainwater, E. L., & Smith, M. S. (2004). Ultra high altitude balloons for medium-to-large payloads. *Advances in Space Research*, 33(10), 1648–1652.
- Smith, D. J., Thakrar, P. J., Bharrat, A. E., Dokos, A. G., Kinney, T. L., James, L. M., ... others. (2014). A balloon-based payload for Exposing Microorganisms in the Stratosphere (E-MIST). *Gravitational and Space Research*, 2(2).
- Smith, M., & Rainwater, L. (2013). Applications of scientific ballooning technology to high altitude airships. In *AIAA's 3rd Annual Aviation Technology, Integration, and Operations (ATIO) Forum* (p. 6711).
- Yagi, H. (1997). Beam Transmission Of Ultra Short Waves. *Proceedings of the IEEE*, 85(11), 1864–1874. <https://doi.org/10.1109/JPROC.1997.649674>
- Yajima, N., Izutsu, N., Imamura, T., & Abe, T. (2009). *Scientific ballooning: Technology and applications of exploration balloons floating in the stratosphere and the atmospheres of other planets. Scientific Ballooning: Technology and Applications of Exploration Balloons Floating in the Stratosphere and the Atmospheres of Other Planets*. <https://doi.org/10.1007/978-0-387-09727-5>
- Yebuah, I. K., & Torkudzor, M. K. (2014). Fabrication and Optimisation of Biquad Antenna for Wireless Local Area Network. In *7th Annual International Applied Research Conference* (pp. 1–8). Koforidua.